# Structural Characterization of the Interactions between Calmodulin and Skeletal Muscle Myosin Light Chain Kinase: Effect of Peptide (576–594)G Binding on the $Ca^{2+}$-Binding Domains†

Steven H. Seeholzer and A. Joshua Wand*

*Institute for Cancer Research, Fox Chase Cancer Center, 7701 Burholme Avenue, Philadelphia, Pennsylvania 19111*

*Received October 27, 1988; Revised Manuscript Received January 12, 1989*

ABSTRACT: Calcium-containing calmodulin (CaM) and its complex with a peptide corresponding to the calmodulin-binding domain of skeletal muscle myosin light chain kinase [skMLCK(576–594)G] have been studied by one- and two-dimensional $^1H$ NMR techniques. Resonances arising from the antiparallel $\beta$-sheet structures associated with the calcium-binding domains of CaM and their counterparts in the CaM–skMLCK(576–594)G complex have been assigned. The assignments were initiated by application of the main chain directed assignment strategy. It is found that, despite significant changes in chemical shifts of resonances arising from amino acid residues in this region upon binding of the peptide, the $\beta$-sheets have virtually the same structure in the complex as in CaM. Hydrogen exchange rates of amide NH within the $\beta$-sheet structures are significantly slowed upon binding of peptide. These data, in conjunction with the observed nuclear Overhauser effect (NOE) patterns and relative intensities and the downfield shifts of associated amide and $\alpha$ resonances upon binding of peptide, show that the peptide stabilizes the $Ca^{2+}$-bound state of calmodulin. The observed pattern of NOEs within the $\beta$-sheets and their structural similarity correspond closely to those predicted by the crystal structure. These findings imply that the apparent inconsistency of the crystal structure with recently reported low-angle X-ray scattering profiles of CaM may lie within the putative central helix bridging the globular domains.

Calmodulin, an acidic protein composed of 148 amino acid residues, binds four $Ca^{2+}$ ions with dissociation constants in the micromolar range. It modulates the activity of many enzymes in response to changes in $Ca^{2+}$ concentration, and a $Ca^{2+}_4$–calmodulin- (CaM)[1] dependent enzyme regulation occurs through a tight binding interaction of CaM with specific domains of the regulated enzymes. CaM-binding domains of myosin light chain kinase, a CaM-regulated enzyme, have been identified and characterized for the smooth (Lukas et al., 1986; Kemp et al., 1987) and skeletal (Blumenthal et al., 1985) muscle enzymes. Properties of these isolated CaM-binding domains and other model peptides with high affinity (greater than $10^8$ $M^{-1}$) for CaM are as follows: they contain predominantly hydrophobic and basic amino acids which have a propensity for helix formation (Cox et al., 1984; McDowell et al., 1985); they appear to adopt a helical conformation while bound to CaM (Geidroc et al., 1983; Maulet & Cox, 1983; Cox et al., 1985; McDowell et al., 1985; Klevit et al., 1985; O'Neil et al., 1987); they bind to calmodulin with high affinity in a calcium-dependent manner; they competitively inhibit CaM-dependent activation (Comte et al., 1983).

Calmodulin has been the subject of a variety of structural studies. In the crystal, it is seen to have a dumbbell-like appearance in which there are two pairs of helix–loop–helix $Ca^{2+}$-binding motifs in each globular domain (Babu et al., 1985, 1987). Each $Ca^{2+}$-binding loop participates in a short antiparallel sheet joining two calcium-binding loops to each other. The two globular domains of calmodulin in the crystal are separated by a long helix formed from the central portion of CaM (residues 65–92). Nuclear magnetic resonance (NMR) techniques have also been applied to study $Ca^{2+}$ binding (Seamon, 1979, 1980; Ikura et al., 1983a; Teleman et al., 1986). Many of the proton resonances have been assigned to specific amino acids in intact CaM in both the $Ca^{2+}$-free (Ikura et al., 1983a) and $Ca^{2+}$-saturated (Ikura et al., 1983b) states. The problem of assigning the $^1H$ NMR spectrum of CaM has been somewhat simplified by the use of tryptic fragments of CaM [CaM(1–75) and CaM(76–148)] (Dalgarno et al., 1984; Ikura et al., 1985, 1987; Ikura, 1986). These tryptic fragments have thus far been found to have similar tertiary structures as their counterparts in intact calmodulin (Aulabaugh et al., 1984).

Calmodulin's interaction with tight binding peptides has been the subject of numerous studies including several $^1H$ NMR studies [e.g., Klevit et al. (1985) and Seeholzer et al. (1986, 1987)]. One such peptide is an integral part of the calmodulin binding domain of the skeletal muscle myosin light chain kinase [skMLCK(576–594)] (Blumenthal et al., 1985). In a recent study of the effects of the binding of skMLCK-(576–594) to calmodulin, significant changes in the confor-

†This work was supported by Instrumentation Grants RR-02497 (NIH) and DMB 84-13986 (NSF), by an award from Marie Z. Cole Montrose, by a grant from the Pew Memorial Trust, by NIH Grants CA-06927 and RR-05539, by an appropriation from the Commonwealth of Pennsylvania awarded to the Institute for Cancer Research, and by NIH Research Grants GM-35940 and DK-39806 awarded to A.J.W. S.H.S. is the recipient of an NIH postdoctoral fellowship (CA-09035) administered by the Institute for Cancer Research.

* Address correspondence to this author at the Institute for Cancer Research.

[1] Abbreviations: CaM, $Ca^{2+}_4$–calmodulin; COSY, *J*-correlated spectroscopy; DQF, double quantum filter; EDTA, ethylenediaminetetraacetic acid; HPLC, high-pressure liquid chromatography; MCD, main chain directed; NMR, nuclear magnetic resonance; NOE, nuclear Overhauser effect; NOESY, NOE-correlated spectroscopy; RCT, relayed coherence transfer; skMLCK, skeletal muscle myosin light chain kinase; TOCSY, total correlation spectroscopy; Tris, tris(hydroxymethyl)-aminomethane. Single- and triple-letter codes for amino acids are used interchangeably throughout the paper.

0006-2960/89/0428-4011$01.50/0 

mation of both the peptide and calmodulin upon complex formation were inferred from the observed changes in one-dimensional $^1H$ NMR spectra (Klevit et al., 1985; Klevit & Blumenthal, 1987). The purpose of the present study is to investigate this phenomenon more completely by applying two-dimensional NMR techniques to assign the resonances arising from the two antiparallel sheets comprising the $Ca^{2+}$-binding domains of calmodulin, to assign the corresponding residues in the CaM–skMLCK(576–594) complex, and to characterize the structures of each. Here we confirm previous resonance assignments of the proton spectrum of intact CaM, make numerous additional assignments, and in parallel, assign the corresponding resonances of the CaM–skMLCK(576–594)G complex. The latter assignments specifically identify numerous resonances downfield from the water resonance which were previously inferred to be $\alpha$-proton resonances of sheet structures on the basis of chemical shift arguments (Klevit et al., 1985; Klevit & Blumenthal, 1987). Structural information concerning the two antiparallel sheets in CaM has been revealed from analysis of the interproton distance information available from 2D NOESY spectra. It is found that the morphologies of the two antiparallel sheets of calmodulin are preserved upon binding of the skMLCK-(576–594) peptide. Binding of this peptide significantly restrains CaM's structural motions as shown by the reduction of amide hydrogen exchange rates throughout the protein upon peptide binding.

## Materials and Methods

*Preparation of Calmodulin.* Calmodulin was isolated and purified by hydrophobic interaction chromatography (Gopalakrishna & Anderson, 1982). Mature *Bos taurus* testicles were homogenized in 50 mM Tris, 1 mM EDTA, and 1 mM $\beta$-mercaptoethanol, pH 7.5. Following centrifugation, the calmodulin was precipitated by adjusting the pH of the supernatant to the isoelectric point of calmodulin (pH 4.3) with acetic acid. Calmodulin was recovered by centrifugation, and after the resulting pellet was resuspended in 50 mM Tris buffer, the pH was readjusted to 7.5 with Tris base. The insoluble material was removed by centrifugation, and 5 mM $CaCl_2$ was added to the supernatant. This supernatant was then passed through a phenyl-Sepharose (Pharmacia) column equilibrated with 50 mM Tris, 1 mM $CaCl_2$, and 1 mM $\beta$-mercaptoethanol, pH 7.5. After the column was washed with this buffer plus 1 M NaCl, the calmodulin was eluted from the column with 1 mM EDTA in 50 mM Tris, pH 7.5. After extensive dialysis against 50 mM $NH_4HCO_3$ and 1 mM $CaCl_2$, the calmodulin was further purified by gel filtration chromatography on a column of Sephadex G-75-SF. The preparation was stored as a lyophilized powder in the $Ca^{2+}$-saturated state. It was judged to be pure by UV spectroscopy, sodium dodecyl sulfate–polyacrylamide gel electrophoresis, and NMR spectroscopy.

*Peptide Synthesis and Purification.* The peptide used in this study, on the basis of the sequence of the skMLCK CaM-binding domain (Blumenthal et al., 1985), is

skMLCK(576–594)G

Ac-M-K-R-R-W-K-K-N-R-F-I-A-V-S-A-A-N-R-F-G-$NH_2$

skMLCK(576–594)G was prepared with an N-terminal-acetylated methionine and a C-terminal glycine amide on an Applied Biosystems automatic peptide synthesizer. Following cleavage and deprotection, the peptide was purified to homogeneity by gel filtration (Sephadex G-10), followed by cation-exchange chromatography (CM-Sephadex C-25, linear $NH_4HCO_3$ gradient), and finally by reverse-phase HPLC on a 1 × 25 cm C-18 column (Waters) with a water–acetonitrile solvent system in the presence of 0.1% trifluoroacetic acid. The final purity of skMLCK(576–594)G was found to be greater than 98% with an analytical C-8 reverse-phase column (Alltech).

*Sample Preparation.* NMR samples were prepared from stock solutions (0.2–1 mM) of CaM and skMLCK(576–594)G obtained by resuspending the lyophilized polypeptide in water and adjusting the pH to 6.5 with dilute KOH or HCl, as necessary. The concentrations of CaM and skMLCK(576–594)G in these stock solutions were determined by UV spectroscopy using extinction coefficients of 3.24 and 5.55 $mM^{-1}$ $cm^{-1}$, respectively. CaM samples for two-dimensional NMR spectroscopy were prepared by adding 1 $\mu$mol of perdeuterated imidazole and 0.05 $\mu$mol of sodium azide to 2 $\mu$mol of CaM and then proceeding with two to three cycles of lyophilization and resuspension in progressively smaller volumes of water. This process was continued until the pH of the sample no longer needed adjustment to 6.5 with dilute KOH or HCl. The sample was made ready for NMR analysis by resuspension of the lyophilized powder in 0.5 mL of 10% $D_2O$ and 90% $H_2O$. CaM–skMLCK(576–594)G (1:1) samples were prepared for analysis by 2D NMR in much the same way; however, the complex was created in the first step by slowly adding 2 $\mu$mol of skMLCK(576–594)G to the CaM. A considerable amount of precipitate results from addition of concentrated solutions of this and other peptides to CaM. By creation of the complex under dilute conditions (ca. 0.1–0.2 mM) and then gradual concentration in the way described for CaM, the amount of precipitant formed upon mixing peptide with CaM is greatly reduced. Samples for the titration of CaM with skMLCK(576–594)G were prepared by first exchanging CaM's amide protons for deuterons at pH 7.5, 50 °C in $D_2O$ for 24 h. The exchanged CaM sample was then split into equal aliquots and 2 equiv of skMLCK(576–594)G (in $D_2O$) added to one aliquot. The samples were then handled as described above except that $D_2O$ was used as solvent. The titration was executed by cross-mixing predetermined amounts of CaM with CaM–skMLCK(576–594)G to sequentially yield the desired CaM:peptide ratios. The concentration of CaM used in these titrations was 0.5 mM.

*NMR Spectroscopy.* All NMR spectra shown were obtained on a Bruker AM 500 NMR spectrometer modified for solvent suppression as described elsewhere (Dykstra, 1987; Dykstra & Wand, 1988). Standard pulse sequences were used for phase-sensitive DQF COSY (Rance et al., 1984), NOESY (Macura & Ernst, 1980), spin-locked TOCSY (Bax & Davis, 1985), and magnitude-mode RCT COSY (Wagner, 1983) experiments. Spectra obtained in $H_2O$ solvent employed the SCUBA sequence of Brown et al. (1988). The sweep width used was 6944 Hz in all cases. Pure absorption spectra were derived from data sets composed of at least 750 $t_1$ increments of 1024 complex data points. Quadrature detection during the incremented time domain of pure absorption mode experiments was achieved by time proportional phase incrementation (Redfield & Kuntz, 1975; Marion & Wüthrich, 1983). All spectra were processed to 2048 × 2048 real points with FTNMR software from Dr. Dennis Hare (Hare Research Inc., Woodinville, WA). All spectra presented here were recorded at 37 °C and are referenced to external (coaxial capillary) sodium 3-(trimethylsilyl)propionate-*2,2,3,3-d*$_4$ at 0.0 ppm.

## Results

*Characterization of the CaM–skMLCK(576–594)G Complex.* The titration of CaM with up to 2 equiv of skMLCK-

(576–594)G was followed by one-dimensional $^1$H NMR spectroscopy. In the presence of substoichiometric amounts of peptide, the $^1$H NMR spectrum is composed of two distinct sets of resonances. One set of resonances is identical with those of free calmodulin while the other set corresponds to the spectrum of the 1:1 CaM–skMLCK(576–594)G complex. The interconversion of free and bound peptide is therefore in slow exchange on the chemical shift time scale.[2] This is expected for ligands with dissociation constants in the nanomolar range. Many $^1$H resonances of CaM and their counterparts in the CaM–skMLCK(576–594)G complex have been assigned (Table I; see below). It is found that the peptide affects the chemical shifts of resonances arising from both the N- and C-terminal domains of CaM. No additional changes in calmodulin resonances upon titration of CaM with more than 1 equiv of skMLCK(576–594)G are observed. The difference spectrum resulting from the subtraction of the spectrum of 1:1 CaM–skMLCK(576–594)G complex from that of the 2:1 mixture closely resembles the spectrum of the uncomplexed skMLCK(576–594)G. However, several minor chemical shift changes and a general broadening of the resonances of the excess peptide are observed (not shown). Together, these data indicate a CaM–skMLCK(576–594)G tight binding stoichiometry of 1 to 1 and an exceedingly weak interaction of excess peptide with calmodulin. These results reaffirm previous observations with two similar peptides (Klevit et al., 1985; Klevit & Blumenthal, 1987).

Two-dimensional $^1$H NMR spectra of CaM and its skMLCK(576–594)G complex revealed several new features of the interaction. The aromatic resonance regions of pertinent DQF COSY spectra are shown in Figure 1. Many of the aromatic side chain spin systems of CaM have been assigned already in intact CaM (Ikura et al., 1983a) and in the tryptic half-fragments of CaM (Dalgarno et al., 1984; Ikura et al., 1985, 1987; Ikura, 1986). The chemical shifts of the two tyrosines are indicated in Figure 1A. The chemical shifts of the two Phe residues and the single Trp residue of skMLCK-(576–594)G in $D_2O$ (Figure 1B) are very close to the chemical shifts of these residues in the "random coil" state (Bundi & Wüthrich, 1979). Upon binding to CaM, the Trp resonances experience large upfield shifts to the new positions indicated in Figure 1C. The benzoid ring spin system of the tryptophan indole ring is shown along with the sequence-specific assignments of Tyr99 and Tyr138. In the complex, the skMLCK-(576–594)G Trp side-chain H2 resonance is degenerate with that of the H7. Other changes in the aromatic region of these spectra upon CaM–skMLCK(576–594)G complex formation are the more subtle downfield and upfield shifts of CaM's Tyr99 and Tyr138 resonances, respectively. Also evident are the appearance of three additional cross peaks in spectral regions previously devoid of cross peaks. These resolved resonances are seen at 7.7, 7.6, and 6.44 ppm in both two- (Figure 1C) and one-dimensional spectra (Figure 2B). Relay COSY and TOCSY spectra (not shown) reveal these peaks to be part of Phe aromatic ring spin systems. We have yet to assign all of these spin systems to specific residues in the primary sequence. However, our work on assigning resonances from skMLCK(576–594)G complexed with perdeuterated CaM indicates that all three of these phenylalanine spin systems arise from calmodulin and not from the bound peptide.[3] Two other calmodulin phenylalanine side-chain resonances are affected by the binding of skMLCK(576–594)G (Figure 1). These have been assigned to Phe16 and Phe89 (Dalgarno et al., 1984). The perturbation is somewhat disguised in the one-dimensional spectrum in which the reso-

Table I: $^1$H Resonance Assignments in the $Ca^{2+}$-Binding Domains of Calmodulin and the CaM–skMLCK(576–594)G Complex[a]

| | chemical shift (ppm) | | | |
|---|---|---|---|---|
| residue | NH | $C_\alpha H$ | $C_\beta H$ | other |
| G23 | 7.70 | | | |
| | (–) | | | |
| D24 | 8.41 | – | – | |
| | (8.52) | (4.55) | (1.64) | |
| G25 | 10.62 | 4.39, 3.72 | | |
| | (10.61) | (4.42, 3.75) | | |
| T26 | 8.17 | 5.33 | 3.87 | 1.07, $\gamma CH_3$ |
| | (8.22) | (5.46) | (3.83) | (1.07), $\gamma CH_3$ |
| I27 | 9.80 | 4.98 | 1.82 | |
| | (9.97) | (4.79) | (1.83) | |
| T28 | 8.52 | 4.85 | 4.83 | 1.33, $\gamma CH_3$ |
| | (8.47) | (4.89) | (4.81) | (1.33), $\gamma CH_3$ |
| T29 | 9.01 | 4.00 | 4.12 | 1.36, $\gamma CH_3$ |
| | (9.14) | (3.73) | (4.20) | (1.29), $\gamma CH_3$ |
| K30 | 8.68 | | | |
| | (8.74) | | | |
| N60 | 8.11 | 4.70 | | |
| | (8.18) | (4.66) | | |
| G61 | 10.58 | 4.22, 3.51 | | |
| | (10.63) | (4.30, 3.52) | | |
| T62 | 7.70 | 4.79 | 4.03 | 1.13, $\gamma CH_3$ |
| | (7.69) | (4.81) | (4.03) | (1.16), $\gamma CH_3$ |
| I63 | 8.91 | 5.18 | 2.09 | 1.25, $\gamma CH_3$ |
| | (8.80) | (5.35) | (2.30) | (1.36), $\gamma CH_3$ |
| D64 | 8.91 | 5.40 | 3.10, 2.86 | |
| | (9.05) | (5.51) | (3.19, 2.87) | |
| F65 | 8.99 | 4.04 | 2.85, 2.41 | 6.64, o; 7.04, m; 7.23, p |
| | (8.95) | (3.96) | (2.83, 2.35) | (7.08, o; 7.28, m; 7.38, p) |
| G98 | 7.79 | | | |
| | (–) | | | |
| N97 | 8.35 | 4.67 | | |
| | (8.44) | (4.42) | | |
| G98 | 10.64 | 4.08, 3.46 | | |
| | (10.72) | (4.14, 3.50) | | |
| Y99 | 7.63 | 5.07 | 2.54, 2.50 | 6.78, o; 6.95, m |
| | (7.71) | (5.09) | (2.60) | (6.79, o; 6.96, m) |
| I100 | 10.16 | 4.84 | 1.90 | 0.98, $\gamma CH_3$ |
| | (10.26) | (4.74) | (2.04) | (–) |
| S101 | 9.01 | 4.88 | 4.46 | |
| | (9.03) | (5.00) | (4.51) | |
| A102 | 9.21 | 3.95 | 1.51 | |
| | (9.31) | (3.96) | (1.55) | |
| A103 | 8.22 | 4.07 | 1.45 | |
| | (8.28) | (4.08) | (1.47) | |
| G132 | 7.60 | 4.01, 3.98 | | |
| | (–) | (–) | | |
| D133 | 8.36 | 4.50 | | |
| | (8.43) | (4.49) | | |
| G134 | 10.35 | 4.06, 3.45 | | |
| | (10.40) | (4.10, 3.50) | | |
| Q135 | 7.98 | 4.90 | 1.72 | |
| | (8.00) | (4.98) | (1.77) | |
| V136 | 9.14 | 5.22 | 2.33 | 1.30, 0.94, $\gamma CH_3$ |
| | (9.14) | (5.22) | (2.38) | (1.13, 1.07, $\gamma CH_3$) |
| N137 | 9.60 | 5.25 | 3.27 | |
| | (9.65) | (5.35) | (3.22) | |
| Y138 | 8.43 | 3.96 | – | 6.32, o; 6.53, m |
| | (8.28) | (3.28) | (3.38, 2.95) | (6.27, o; 6.50, m) |
| E139 | – | – | – | |
| | (8.06) | (3.63) | (2.09) | |

[a] Chemical shifts referenced to external 3-(trimethylsilyl)-propionate-*2,2,3,3-d*$_4$ (coaxial capillary) at 37 °C and pH 6.5. Values for the CaM–skMLCK(576–594)G complex are enclosed in parentheses.

[2] An upper limit for the off-rate of bound skMLCK(576–594)G of 1 $s^{-1}$ can be determined from the observed shifts, in CaM and in the complex, of the trimethyl resonance arising from the posttranscriptionally modified lysine-115 of calmodulin.

[3] Seeholzer and Wand, unpublished results.

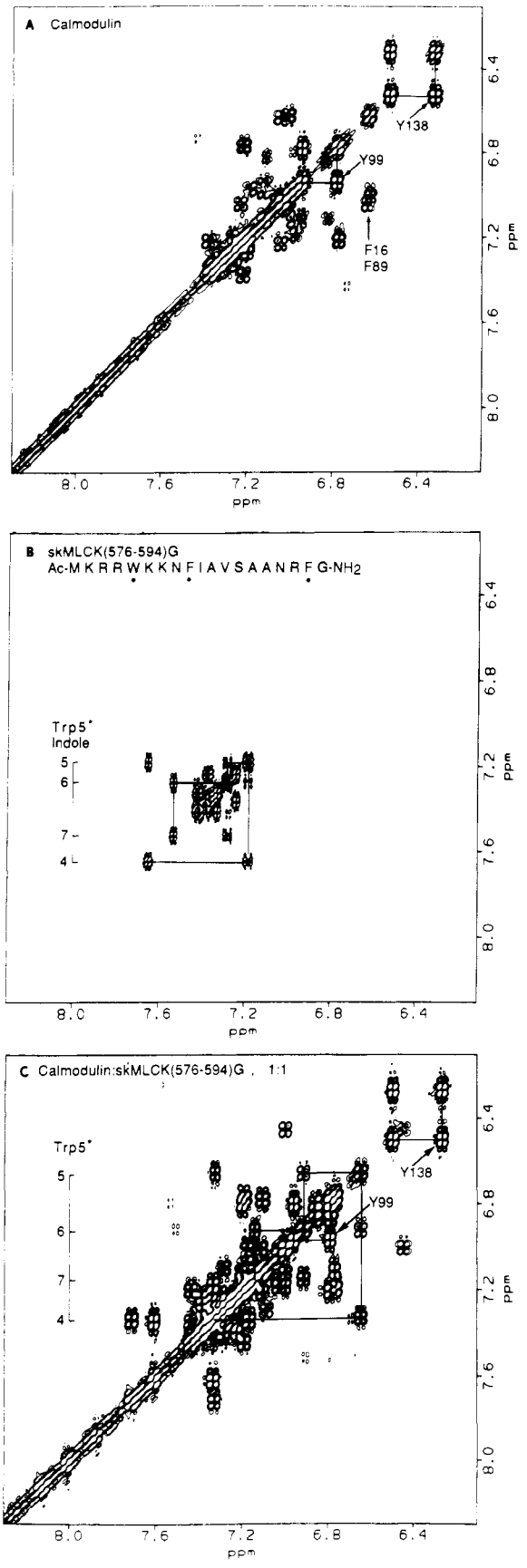


FIGURE 1: Expansions of DQF COSY spectra of CaM in $H_2O$ (panel A), the skMLCK(576–594)G peptide in $D_2O$ (panel B), and the CaM–skMLCK(576–594)G complex in $H_2O$ (panel C). Shown are the aromatic resonance regions of each spectrum. The resonances associated with the single Trp (denoted by asterisks) of the peptide (panel B) shift upon binding of the peptide (panel C).

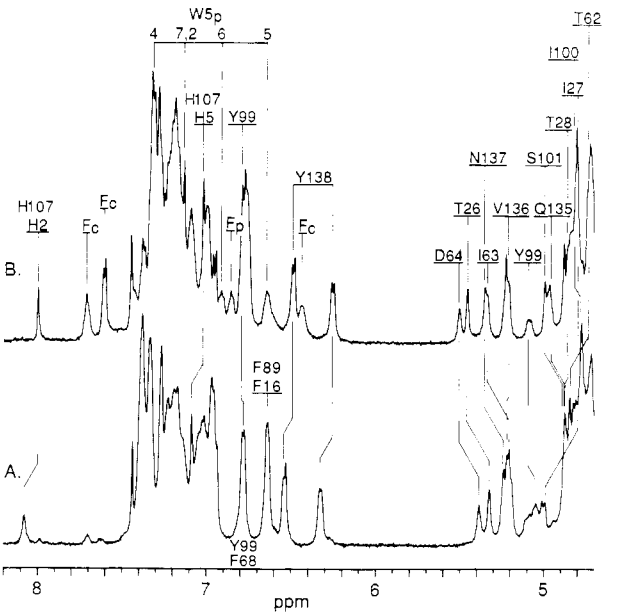


FIGURE 2: Expansions of one-dimensional spectra of CaM (bottom spectrum) and the 1:1 CaM–skMLCK(576–594)G complex (top spectrum). Assignments in CaM and their counterparts in the complex are indicated. Resonances assigned to three phenylalanine ring spin systems of CaM but not assigned to specific sequence positions are indicated as $F_c$, and the resolved peptide Phe resonance is indicated as $F_p$. The resonances arising from the Trp residue of the peptide are indicated as $W5_p$. See text for discussion.

nances of Phe16 and Phe89 at 6.65 ppm in calmodulin (Figure 2A) appear to become broadened in the presence of skMLCK(576–594)G. In fact, as the two-dimensional spectra clearly show, these resonances shift out of this region and are replaced by the Trp H5 resonance of the bound peptide.

The effects of skMLCK(576–594)G on the various CaM resonances discussed above have been illustrated solely with the behavior of side-chain resonances of calmodulin. Hence, these effects can be interpreted only so far as to indicate CaM side-chain rearrangements upon complex formation with skMLCK(576–594)G. The data presented so far do not address main chain secondary or tertiary structure changes. Figure 2 shows one-dimensional spectra from the titration of CaM with skMLCK(576–594)G. The spectra of CaM and 1:1 CaM–skMLCK(576–594)G are shown in panels A and B of Figure 2, respectively. These spectra, part of the titration series mentioned above, summarize the effect of peptide binding on the various aromatic resonances mentioned above. Also shown are the downfield-shifted $\alpha$-protons between 4.8 and 5.5 ppm. Most of these resonances, indicated for both the free CaM (Figure 2A) and for the 1:1 CaM–skMLCK-(576–594)G complex (Figure 2B), are assigned below to one or the other of calmodulin's antiparallel sheets. These spectra are shown to illustrate that significant changes in the chemical shifts of many aromatic and some main chain resonances occur upon formation of the CaM–skMLCK(576–594)G complex. Such chemical shift changes in main chain protons have been cited as evidence for secondary or tertiary structural changes (Klevit et al., 1985; Klevit & Blumenthal, 1987). However, as shown below, the effect is in fact the opposite; preexisting secondary structures associated with the perturbed main chain resonances are stabilized.

*Resonance Assignments of CaM and CaM–skMLCK-(576–594)G.* As mentioned above, many resonances of calmodulin are affected by both $Ca^{2+}$ binding and by peptide binding to CaM (Figures 2–4). Some of these have been assigned by others to the calcium-binding domains of calmo-

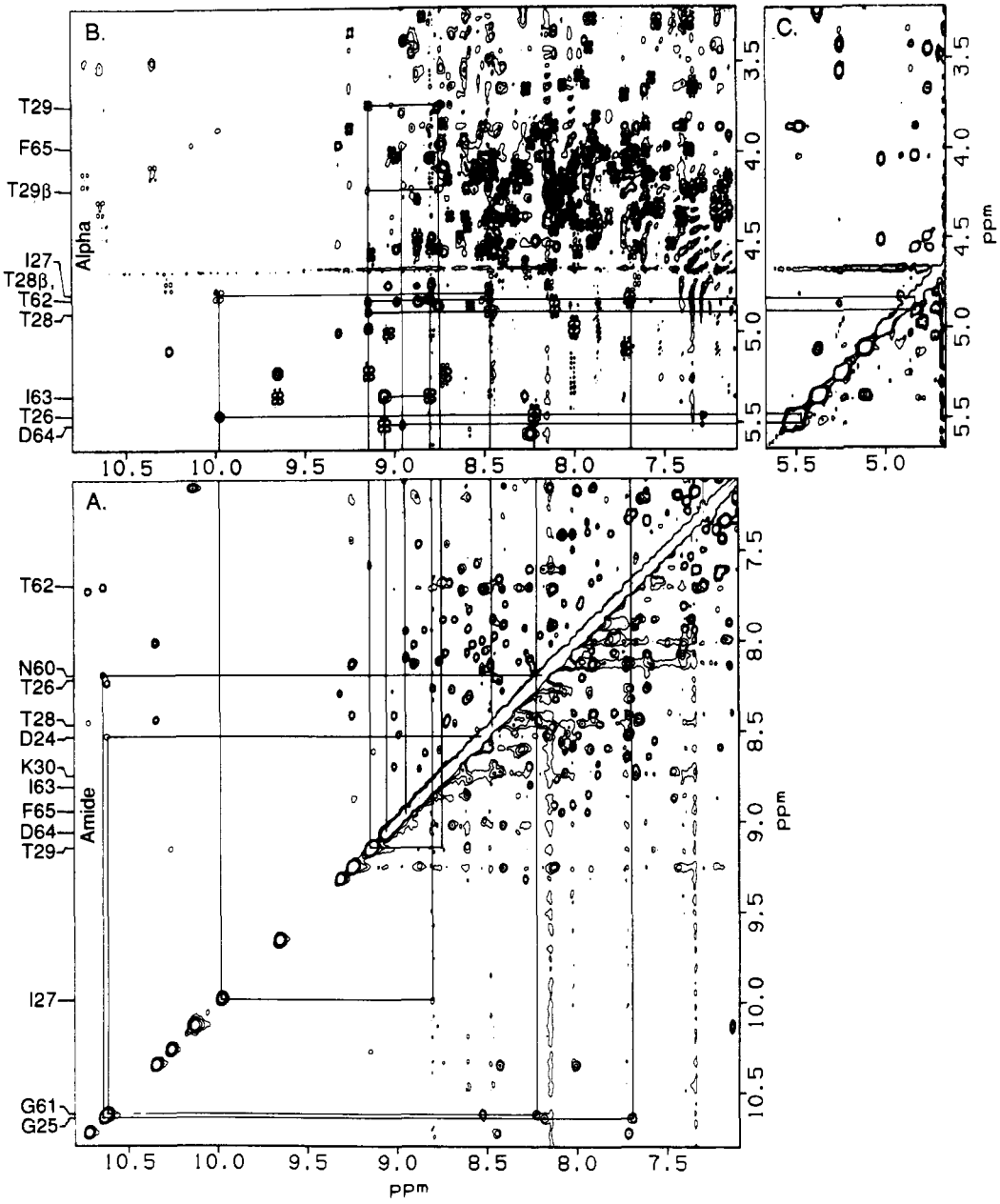


FIGURE 3: Expansions of NOESY spectra obtained in $H_2O$ (panels A and B) and $D_2O$ (panel C) of the 1:1 CaM–skMLCK complex. The $H_2O$ DQF COSY spectrum is superimposed in panel B. Shown are the NOE connectivities used to define the N-terminal antiparallel sheet region of calmodulin in the CaM–skMLCK(576–594)G complex (see text). The mixing time used was 80 ms. The NOE connectivities used are schematically summarized in Figure 5.

dulin. Such effects of $Ca^{2+}$ binding are therefore not unexpected. An effect of peptide binding on these regions, however, is not necessarily expected. In order to examine such effects, we have confirmed and greatly extended the resonance assignments of residues in the two antiparallel sheets of CaM and demonstrate the existence of the two antiparallel $\beta$-sheets in the 1:1 CaM–skMLCK(576–594)G complex. The assignment was initiated by the application of the main chain directed assignment (MCD) algorithm (Englander & Wand, 1987; Di Stefano & Wand, 1987; Wand & Nelson, 1989). Amide NH–$C_\alpha$H–$C_\beta$H $J$-coupled subspin systems were obtained from analysis of DQF COSY, RCT COSY, and TOCSY spectra of calmodulin and the CaM–skMLCK(576–594)G complex. Potential antiparallel sheet-like structures were searched for in NOESY spectra with the so-called inner, outer, and hybrid MCD patterns (Englander & Wand, 1987; Wand & Nelson, 1989). Ultimately, two antiparallel sheet structures were to be found represented in NOESY spectra of both CaM and the CaM–skMLCK(576–594)G complex (Figures 3 and 4). In all cases, the sheet-like structures were defined by the hybrid pattern which displays the lowest fidelity of the three fundamental antiparallel sheet MCD patterns sought (Englander & Wand, 1987; Wand & Nelson, 1989). However, these MCD-defined structures contain several particularly simple amino acid side chains (e.g., Gly, Thr, and Ala) which allowed the obtained MCD patterns to be unequivocally aligned with the primary sequence. In both CaM and the CaM–skMLCK(576–594)G complex the $\beta$-sheets involve residues 26–29 and 62–65 in the N-terminal half of CaM and residues 99–102 and 135–138 in the C-terminal half. This is in agreement with the crystal structure of CaM (Babu et al., 1985). Furthermore, despite the extensive change of chemical shifts observed for the residues involved in the antiparallel sheets, the main chain NOE patterns and relative intensities are found to change very little upon binding of the skMLCK peptide to CaM. It is interesting to note that

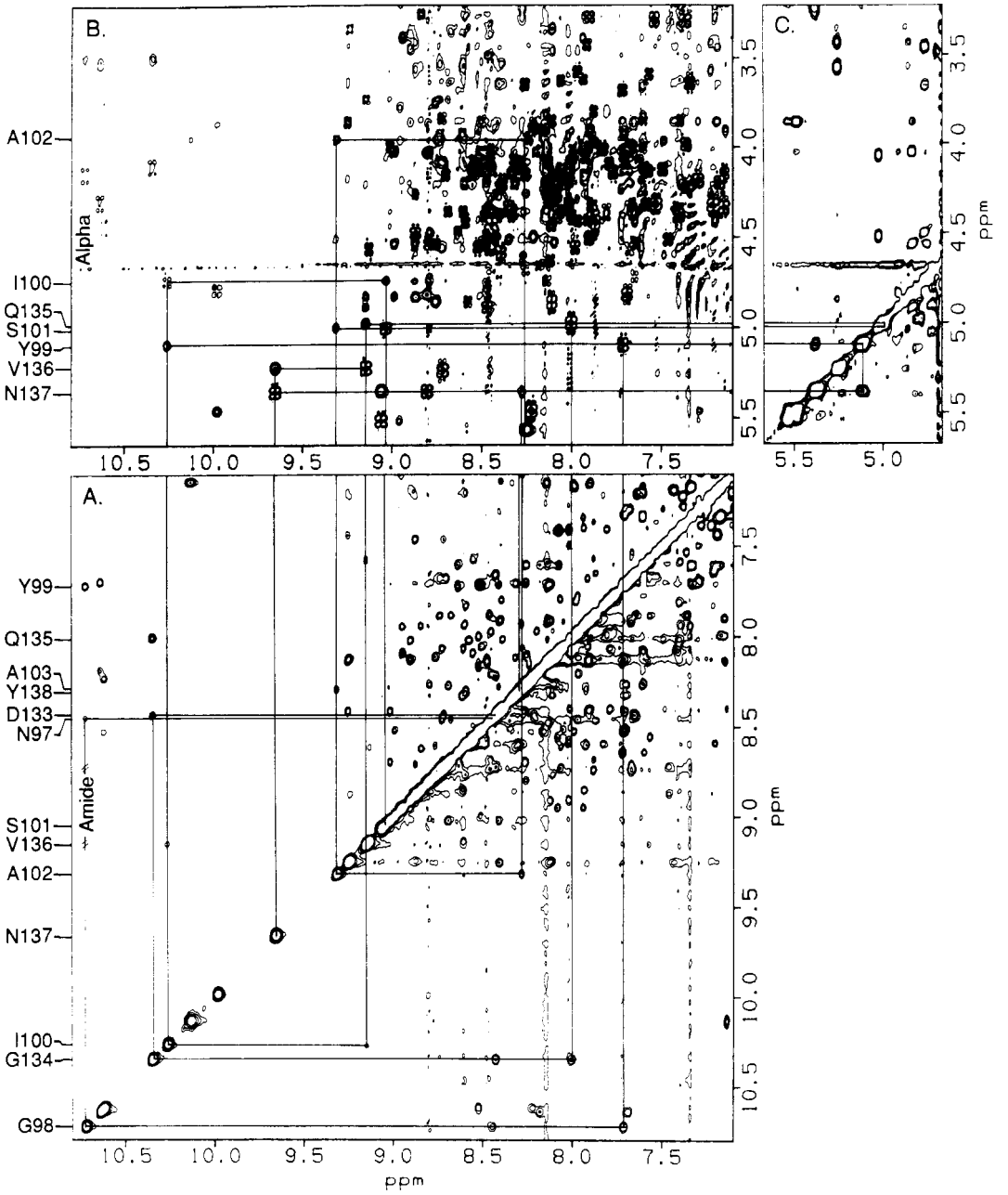


FIGURE 4: Expansions of NOESY spectra obtained in $H_2O$ (panels A and B) and $D_2O$ (panel C) of the 1:1 CaM–skMLCK complex. The $H_2O$ DQF COSY spectrum is superimposed in panel B. Shown are the NOE connectivities used to define the C-terminal antiparallel sheet region of calmodulin in the CaM–skMLCK(576–594)G complex (see text). The mixing time used was 80 ms. The NOE connectivities used are schematically summarized in Figure 5.

helical-like MCD patterns (Englander & Wand, 1987; Wand & Nelson, 1989) are seen leading from both sheets in calmodulin, in agreement with the crystal structure (Babu et al., 1985), and persist in the CaM–skMLCK(576–594)G complex (not shown). Assigned resonances in CaM and the CaM–skMLCK(576–594)G complex are summarized in Table I.

Figures 3 and 4 show expanded regions of phase-sensitive NOESY spectra of the CaM–skMLCK(576–594)G complex. Corresponding amide–$\alpha$ regions of a phase-sensitive DQF COSY spectrum are superimposed on the NOESY spectra in Figures 3B and 4B. DQF COSY cross peaks can be distinguished from the NOESY cross peaks in Figures 3B and 4B by their resolved multiplet fine structure. Main chain scalar (through bond) and dipolar (through space) connectivities are indicated by lines drawn in Figure 3 for CaM's N-terminal $Ca^{2+}$-binding domain and in Figure 4 for CaM's C-terminal $Ca^{2+}$-binding domain. There is a close correspondence of NOE contacts between protons in one domain and their homologues in the other domain. This is more clearly illustrated by Figure 5 which gives a schematic summary of the main chain NOE contacts in the N-terminal (Figure 5A) and C-terminal (Figure 5B) antiparallel sheet regions of CaM's $Ca^{2+}$-binding domains. Curved arrows represent intraresidue connectivities established from *J*-correlated data (i.e., DQF COSY shown in Figures 3B and 4B), and straight arrows indicate interresidue NOE contacts found in the NOESY spectra given in Figures 3 and 4. Hybrid antiparallel sheet MCD NOE patterns are seen between residues T26–T29 and T62–F65 in the N-terminal domain and between residues Y99–A102 and Q135–Y138. Missing are the cross-strand amide–$\alpha$ NOEs expected for ideal antiparallel sheets (Englander & Wand, 1987; Wand & Nelson, 1989). This is consistent with the extensive twist of the sheets observed in the crystal structure (Babu et al., 1985). Not shown are the helical MCD NOE patterns found to begin

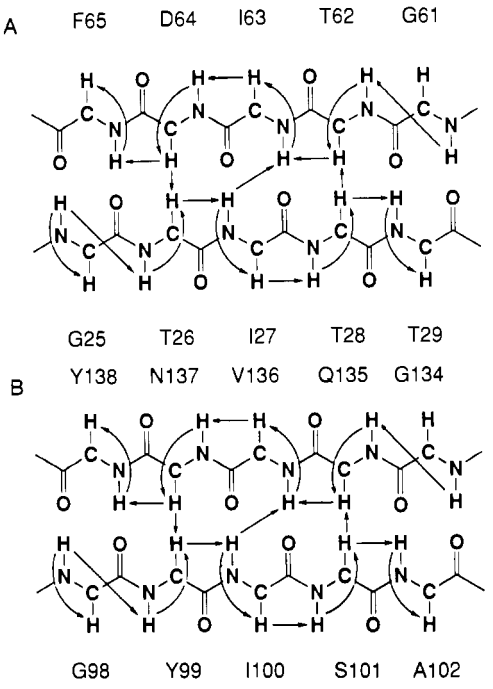


FIGURE 5: Schematic summary of the NOE connectivities (straight arrows) and *J*-coupled connectivities (curved arrows) used in the construction of MCD patterns defining the N-terminal (A) and C-terminal (B) antiparallel sheets of calmodulin in the CaM–skMLCK(576–594)G complex. Note the correspondence of NOEs between the two domains. The same combination and relative intensities of NOEs are observed for free calmodulin (see text).

at residues T29, A102, and Y138 involving amide–amide and $\beta$–amide NOEs. One striking feature of this figure is the remarkable symmetry of the NOE interactions between the N- and C-terminal antiparallel sheets. Such symmetry is also observed in the crystal structure of CaM (Babu et al., 1985). Most important is that the same combination and relative intensities of NOEs are observed for these two regions in the calmodulin (Figures S1 and S2 of the supplementary material). It should be noted that preliminary progress curves of the NOE as a function of mixing time indicate spin diffusion is not significant at the mixing times used here. Thus the observed NOEs remain a semiquantitative measure of the indicated distance relationships.

*Structural Dynamics.* We have previously observed that melittin binding to CaM dramatically alters the structural dynamics of the protein as evidenced by rather large effects of peptide binding on the rate of amide hydrogen exchange with the solvent (Seeholzer et al., 1986). Similar effects are also observed upon the binding of skMLCK(576–594)G to CaM. Figure 6 shows the fingerprint region of the phase-sensitive DQF COSY spectra of CaM (Figure 6A) and the CaM–skMLCK(576–594)G complex (Figure 6B) in $D_2O$. Both of these spectra were recorded approximately 34 h after the addition of $D_2O$ to the lyophilized samples and are plotted at similar levels. Whereas only one amide hydrogen atom remains incompletely exchanged in the CaM spectrum (Figure 6A), 34 NH–$\alpha$ cross peaks are clearly visible in the spectrum of CaM–skMLCK(576–594)G (Figure 6B). Fourteen of these NH-$\alpha$ cross peaks arise from residues assigned to the $Ca^{2+}$-binding domains of CaM (i.e., 26–29, 62–64, 99–102, and 135–137). The amides of Tyr138 and Phe65 are not sufficiently stabilized to be observed under the conditions used here (Figure 6B). It is interesting to note that these two residues occupy homologous positions at the ends of the antiparallel sheets. Many of the remaining NH–$C_\alpha$H cross peaks, which arise from trapped amides in the complex, participate in helical MCD patterns (not shown) and presumably represent residues located in the extensive helical regions of calmodulin. Thus, insofar as a decrease in hydrogen exchange rate for backbone amide hydrogen represents a stabilization of structure (Englander & Kallenbach, 1984), it would appear as if the binding of the skMLCK peptide to calmodulin dampens motions that lead to hydrogen exchange throughout a large portion of the protein.

## Discussion

Previous sequence-specific assignments have been greatly facilitated by the use of the tryptic fragments, the most extensive assignments having been made by studying the C-terminal domain of scallop (*Patinopectin* sp.) CaM (Ikura et al., 1985). We have chosen to work with intact calmodulin since it is clear that many CaM-regulated enzymes are activated only by the intact CaM molecule and not by its tryptic half-fragments (Newton et al., 1984; Minowa et al., 1988). We have extended the assignments made by Ikura and coworkers to intact bovine CaM; after accounting for a systematic difference of 0.03 ppm, about 90% of the chemical shifts are within 0.04 ppm of those determined by Ikura et al. (1985). (Not including resonances arising from residues 97 and 99 which differ between the two species.) The largest difference is found for the $\alpha$-proton resonance of Tyr138. This may be indirectly due to the aforementioned species-sequence differences, which are in the strand of the $\beta$-sheet opposing Tyr138. This resonance also experiences a very large upfield shift (−1.58 ppm) as the C-terminal domain becomes occupied with $Ca^{2+}$ (Ikura et al., 1985).

In addition to confirming and extending resonance assignments of the C-terminal calcium-binding domain of *intact* CaM, we have also assigned de novo the analogous residues in the N-terminal calcium-binding domain of CaM. These latter assignments are largely consistent with the sequence-specific side-chain assignments available from previous studies using tryptic fragments (Ikura et al., 1987). The assignment process was initiated by the application of main chain directed connectivity patterns, thereby allowing us to focus on antiparallel sheet structures without the need for considering the relevant spectra in their entirety. This was a significant advantage, as both the *J*-correlated and NOE-correlated spectra are quite complicated in a system of this size (148 amino acids). The corresponding resonances in the CaM–skMLCK(576–594)G complex (167 amino acids) were also assigned. The MCD patterns used in the assignment define the secondary structure of this region of both CaM and the CaM–skMLCK(576–594)G complex. Schematic summaries of the relevant main chain connectivities used for the assignment of the involved residues are shown in Figure 5. It should be emphasized that these figures are not intended to portray three-dimensional structure but rather to emphasize the secondary structure determined by the semiquantitative distance constraints inferred from the observed NOEs. The definition of boundaries of secondary structure by the MCD patterns found are consistent with the crystal structure (Babu et al., 1985). A striking similarity to the crystal structure is the high degree of symmetry of the observed short distances in the N- and C-terminal domains of CaM in solution.

In spite of the significant changes of resonance positions in CaM upon binding of skMLCK(576–594)G (Table I), we find very little if any evidence for main chain secondary structure changes in the portion of CaM's $Ca^{2+}$-binding domains associated with the assigned resonances. The NOE connectivities in this region of the CaM–skMLCK(576–594)G complex are virtually identical with their counterparts in free CaM (Figure

5). The structural similarity between the N- and C-terminal antiparallel sheets in CaM is also preserved in the presence of skMLCK(576–594)G. The binding of peptide to CaM (Table I) and the binding of $Ca^{2+}$ to apocalmodulin-(78–148) (Ikura et al., 1985) both result in upfield and downfield shifts of resonances. A pairwise comparison of these effects on the amide proton and $\alpha$-proton resonances of corresponding hydrogens in the C-terminal antiparallel sheet shows that all but two of the peptide-induced changes in chemical shift occur in the same direction as the $Ca^{2+}$-induced changes but are of smaller magnitude. (Tyr99 is not considered here since there is a Phe residue in this position in scallop CaM.) These parallel effects of $Ca^{2+}$ and skMLCK(576–594)G on chemical shifts in the $Ca^{2+}$-binding regions of CaM correlate well with the observation that several peptides increase the affinity of CaM for $Ca^{2+}$ (Olwin et al., 1984; Suko et al., 1986). Unfortunately, as illustrated above, it is difficult to ascribe precise structural significance to chemical shift changes in the absence of additional information.[4]

However, in the present study, a marked reduction in the rate of exchange of a significant number of amide hydrogens upon binding of peptide was observed (cf. Figure 6). The exchange rates of all amide NH assigned to hydrogen-bonded residues in the antiparallel sheet regions of the CaM–skMLCK(576–594) are significantly slower than those in uncomplexed calmodulin. In addition, many more as yet unidentified amide protons in calmodulin's helical regions also experience a significant slowing of their hydrogen exchange rates upon binding of peptide to calmodulin. It should be pointed out that, relative to proteins of similar size and thermodynamic stability, the degree of slowing of hydrogen exchange rates is unusually small for CaM rather than unusually large for the complex [see Englander and Kallenbach, (1984)]. Amide hydrogens in proteins exhibit slowed exchange behavior, relative to their peptide rate in free peptide, by virtue of their participation in hydrogen bonding (Englander & Kallenbach, 1984). The amide NH involved in interstrand hydrogen bonding are Ile27, Ile63, Ile100, and Val136. The observed slowing of exchange of these hydrogen-bonded amides is easily explained by an overall increase in the stability of the antiparallel sheet regions of the $Ca^{2+}$-binding domains. Such an increase in stability, derived from the decrease in free energy that is associated with complex formation, would lead to less frequent and/or less significant internal motions, giving rise to hydrogen-bond breakage and subsequent exchange with solvent. The hydrogen exchange data reinforces the interpretation of the chemical shift changes discussed above, and a general stabilization of the antiparallel sheets by the binding of peptide is indicated.

More difficult to explain is a similar peptide-induced decrease in exchange rates of those amide hydrogens located on the outside edges of the antiparallel sheets. The residues involved are T26, T28, T62, and D64 in the N-terminal domain and Y99, S101, Q135, and N137 in the C-terminal domain. We have insufficient spectral assignments of the CaM–skMLCK(576–594)G complex to conclusively identify the hydrogen-bond acceptors for these amide NH using NMR data alone. However, since it was shown above that the binding of peptide has little or no effect on the conformation of much of the calcium-binding domains, it would seem justifiable to use the crystal structure of CaM to identify the potential H-bond acceptors. The crystal structure indicates that the amide NH N-terminal to the interstrand H-bonds discussed above (i.e., T26, T62, Y99, and Q135) are hydrogen bonded to the side-chain oxygen atoms of the corresponding $i - 2$ residue (i.e., D24, N60, N97, and D133, respectively), and the amide NH C-terminal to the interstrand H-bonds (i.e., T28, D64, S101, and N137) are hydrogen bonded to side-chain oxygen atoms of the corresponding $i + 3$ residues (i.e., Glu31, Glu67, Glu104, and Glu140, respectively). The remaining two stabilized amide protons which have been assigned (Asn97 and Asp133) are in the C-terminal $Ca^{2+}$-binding domain but not in antiparallel sheet structures and are hydrogen bonded to side-chain oxygen atoms of Asp95 and Asp131, respectively. The corresponding amide hydrogens in the N-terminal domain are not detectably stabilized by peptide binding under the experimental conditions used. It is interesting to note that all

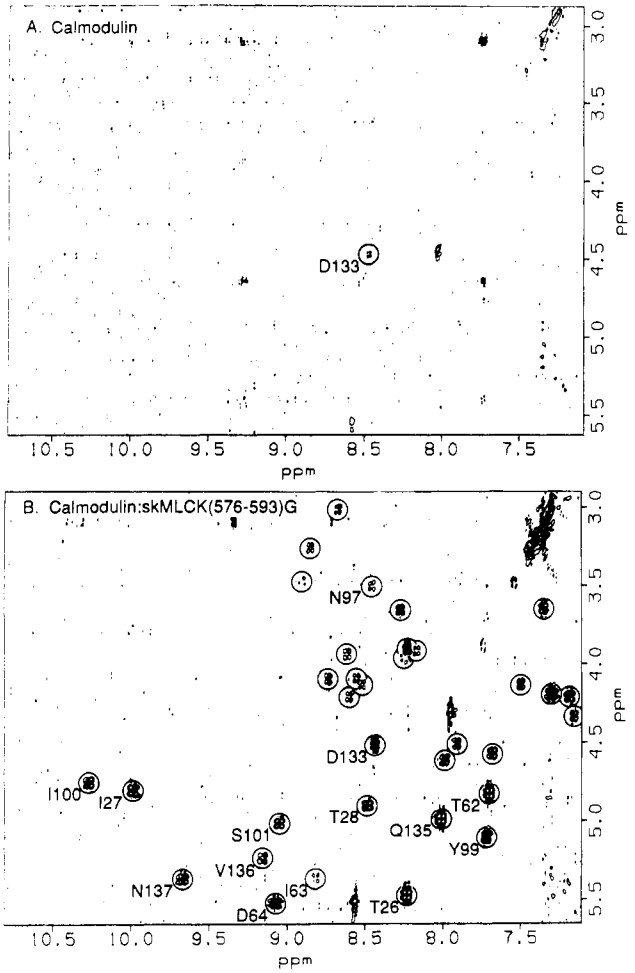


FIGURE 6: Expansions of the fingerprint region of DQF COSY spectra obtained after the addition of $D_2O$ solvent to (A) CaM and (B) the CaM–skMLCK(576–594)G complex. The exchange was carried out at pH 6.5 at room temperature. Both were obtained 34 h after the initiation of hydrogen exchange and are plotted at similar levels.

[4] Increasing hydrogen-bond strength (shorter distance) in $\beta$-sheet structures has been correlated with downfield chemical shifts of involved amide proton and $\alpha$-proton resonances (Wagner et al., 1983). Thus it is interesting to note that most of the chemical shift effects of the binding of peptide on the amide proton and $\alpha$-proton resonances of the antiparallel sheets are in the downfield direction. Following the correlation of Wagner et al. (1983), this would suggest that these changes arise from a stabilization or tightening of the calmodulin's calcium-bound state rather than a conversion to a significantly different secondary structure having a higher affinity for $Ca^{2+}$. The observed downfield shifts, if solely due to the proposed shortening of H-bonds, would entail relative main chain atom movements significantly less than 1 Å [see Wagner et al. (1983)]. This is consistent with the observed NOEs in CaM and in the complex. We have not studied in detail the effect of peptide on apocalmodulin since Klevit et al. (1985) have shown that apocalmodulin and the skMLCK calmodulin binding domain peptide do not interact with one another in the absence of $Ca^{2+}$.

10 of these amino acid residues are known to be involved in liganding for the $Ca^{2+}$ ions (Babu et al., 1985, 1987). Hence, we are directly observing a close correspondence between the peptide-induced stabilization of CaM's structure and the previously observed decrease in the off-rate for $Ca^{2+}$ in the presence of various peptides and target proteins (Olwin et al., 1984; Suko et al., 1986). In the context of the hydrogen exchange results, this represents a case of functional labeling (Englander, 1975) where the change in free energy associated with complex formation is directly reflected in the hydrogen exchange behavior of the amide NH of functionally relevant residues.

Recently, the correspondence of the global character of calmodulin's reported crystal structure to its solution structure has been questioned by the observation that low-angle X-ray scattering profiles are inconsistent with an extended dumbbell structure (Heidorn & Trewhella, 1988). Modeling of the X-ray solution scattering data led to the conclusion that if the globular domains maintain the same structure in solution as that observed in the crystal, then the distances between the two domains must be significantly smaller than that observed in the crystal. This would imply a significant distortion of the long $\alpha$-helix joining the two domains in the crystal (Heidorn & Trewhella, 1988). The structural information presented here lends further credence to the assumption that the globular domains retain the same structure in solution as in the crystal. Further assignment work is necessary to verify this inference that the difference between the solution and crystal structures of calmodulin does indeed reside within the putative central helix bridging the two domains. Such work is in progress.

## Acknowledgments

We gratefully acknowledge Dr. Daniel Hansburg and John Misczak for the synthesis of the peptide used in these studies and Dr. S. Walter Englander and Godfrey Louie for their assistance in purification of the peptide by HPLC. We also gratefully acknowledge Dr. William J. Cook for providing us with atomic coordinates, refined to 2.2 Å, for the crystal structure of calmodulin. We thank Mary Williamson for careful preparation of the manuscript.

## Supplementary Material Available

Two figures of NOESY and DQF COSY spectra of uncomplexed CaM showing the NOE and $J$-coupled connectivities used in the definition of the N- and C-terminal antiparallel sheets (3 pages). Ordering information is given on any current masthead page.

**Registry No.** skMLCK, 51845-53-5; skMLCK(576–594)G, 119391-21-8; Ca, 7440-70-2.

## References

Aulabaugh, A., Niemczura, W. P., & Gibbons, W. A. (1984) *Biochem. Biophys. Res. Commun. 118*, 225–232.

Babu, Y. S., Sack, J. S., Greenbough, T. J., Bugg, C. E., Means, A. R., & Cook, W. J. (1985) *Nature (London) 315*, 37–40.

Babu, Y. S., Bugg, C. E., & Cook, W. J. (1987) in *Calcium-Binding Proteins in Health & Disease*, pp 305–311, Academic Press, New York.

Bax, A., & Davis, D. G. (1985) *J. Magn. Reson. 65*, 355–360.

Blumenthal, D. K., Takio, K., Edelman, A. M., Charbonneau, H., Titani, K., Walsh, K. A., & Krebs, E. G. (1985) *Proc. Natl. Acad. Sci. U.S.A. 82*, 3187–3191.

Brown, S. C., Weber, P. L., & Mueller, L. (1988) *J. Magn. Reson. 77*, 166–169.

Bundi, A., & Wüthrich, K. (1979) *Biopolymers 18*, 285–297.

Comte, M., Maulet, Y., & Cox, J. A. (1983) *Biochem. J. 207*, 269–272.

Cox, J. A., Comte, M., Fitton, J. E., & DeGrado, W. F. (1985) *J. Biol. Chem. 260*, 2527–2534.

Dalgarno, D. C., Klevit, R. E., Levine, B. A., Williams, R. J. P., Dobrowolski, Z., & Drabikowski, W. (1984) *Eur. J. Biochem. 138*, 281–289.

Di Stefano, D. L., & Wand, A. J. (1987) *Biochemistry 26*, 7272–7281.

Dykstra, R. W. (1987) *J. Magn. Reson. 72*, 162–167.

Dykstra, R. W., & Wand, A. J. (1987) *J. Magn. Reson. 75*, 158–161.

Englander, S. W. (1975) *Ann. N.Y. Acad. Sci. 244*, 10–27.

Englander, S. W., & Kallenbach, N. R. (1984) *Q. Rev. Biophys. 16*, 521–655.

Englander, S. W., & Wand, A. J. (1987) *Biochemistry 26*, 5953–5958.

Geidroc, D. P., Ling, N., & Puett, D. (1983) *Biochemistry 22*, 5584–5591.

Gopalakrishna, R., & Anderson, W. B. (1982) *Biochem. Biophys. Res. Commun. 104*, 830–836.

Heidorn, D. B., & Trewhella, J. (1988) *Biochemistry 27*, 909–915.

Ikura, M. (1986) *Biochim. Biophys. Acta 872*, 195–200.

Ikura, M., Hiraoki, T., Hikichi, K., Mikuni, T., Yazawa, M., & Yagi, K. (1983a) *Biochemistry 22*, 2568–2572.

Ikura, M., Hiraoki, T., Hikichi, K., Mikuni, T., Yazawa, M., & Yagi, K. (1983b) *Biochemistry 22*, 2573–2579.

Ikura, M., Minowa, O., & Hikichi, K. (1985) *Biochemistry 24*, 4264–4269.

Ikura, M., Minowa, O., Yazawa, M., Yagi, K., & Hikichi, K. (1987) *FEBS Lett. 219*, 17–21.

Kemp, B. E., Pearson, R. B., Guerriero, V., Jr., Bagchi, I. C., & Means, A. R. (1987) *J. Biol. Chem. 262*, 2542–2548.

Klevit, R. E., & Blumenthal, D. K. (1987) in *Calcium-Binding Proteins in Health & Disease*, pp 333–345, Academic Press, New York.

Klevit, R. E., Blumenthal, D. K., Wemmer, D. E., & Krebs, E. G. (1985) *Biochemistry 24*, 8152–8157.

Lucas, T. J., Burgess, W. H., Prendergast, F. G., Lau, W., & Watterson, D. M. (1986) *Biochemistry 25*, 1458–1464.

Macura, S., & Ernst, R. R. (1980) *Mol. Phys. 41*, 95–117.

Marion, D., & Wüthrich, K. (1983) *Biochem. Biophys. Res. Commun. 113*, 967–974.

Maulet, Y., & Cox, J. A. (1983) *Biochemistry 22*, 5680–5686.

McDowell, L., Sanyal, G., & Prendergrast, F. G. (1985) *Biochemistry 24*, 2974–2984.

Minowa, O., Yazawa, M., Sobue, K., Ito, K., & Yagi, K. (1988) *J. Biochem. 103*, 531–536.

Newton, D. L., Oldewurtel, M. D., Krinks, M. H., Shiloach, J., & Klee, C. B. (1984) *J. Biol. Chem. 259*, 4419–4426.

Olwin, B. B., Edelman, A. M., Krebs, E. G., & Storm, D. R. (1984) *J. Biol. Chem. 259*, 10949–10955.

O'Neil, K. T., Wolfe, H. R., Jr., Erickson-Viitanen, S., & DeGrado, W. F. (1987) *Science 236*, 1454–1456.

Rance, M., Sorensen, O. W., Bodenhausen, G., Wagner, G., Ernst, R. R., & Wüthrich, K. (1984) *Biochem. Biophys. Res. Commun. 117*, 479–485.

Redfield, A. G., & Kuntz, S. D. (1975) *J. Magn. Reson. 19*, 250–254.

Seamon, K. B. (1979) *Biochem. Biophys. Res. Commun. 86*, 1256–1265.

Seamon, K. B. (1980) *Biochemistry 19*, 207-215.
Seeholzer, S. H., Cohn, M., Putkey, J., Means, A. R., & Crespi, H. L. (1986) *Proc. Natl. Acad. Sci. U.S.A. 83*, 3634-3638.
Seeholzer, S. H., Cohn, M., Wand, A. J., Crespi, H. L., Putkey, J. A., & Means, A. R. (1987) in *Calcium-Binding Proteins in Health and Disease*, pp 360-371, Academic Press, New York.
Suko, J., Wyskovsky, W., Pidlich, J., Hauptner, R., Plank, B., & Hellman, G. (1986) *Eur. J. Biochem. 159*, 425-434.
Teleman, A., Drakenberg, T., & Forsen, S. (1986) *Biochim. Biophys. Acta 873*, 204-213.
Wagner, G. (1983) *J. Magn. Reson. 55*, 151-156.
Wagner, G., Pardi, A., & Wüthrich, K. (1983) *J. Am. Chem. Soc. 105*, 5948-5949.
Wand, A. J., & Nelson, S. J. (1989) in *NMR and X-ray Crystallography: Interfaces and Challenges* (Etter, M. C., Ed.) AIP, New York (in press).

# Calcium Affects the Spontaneous Degradation of Aspartyl/Asparaginyl Residues in Calmodulin†

Irene M. Ota and Steven Clarke*

*Department of Chemistry and Biochemistry and the Molecular Biology Institute, University of California, Los Angeles, California 90024*

*Received September 16, 1988; Revised Manuscript Received January 19, 1989*

ABSTRACT: We have previously shown that the D-aspartyl/L-isoaspartyl protein carboxyl methyltransferase recognizes two major sites in affinity-purified preparations of bovine brain calmodulin that arise from spontaneous degradation reactions. These sites are derived from aspartyl residues at positions 2 and 78, which are located in apparently flexible regions of calmodulin. We postulated that this flexibility was an important factor in the nonenzymatic formation and enzymatic recognition of D-aspartyl and/or L-isoaspartyl residues. Because removal of $Ca^{2+}$ ions from this protein may also lead to increased flexibility in the four $Ca^{2+}$ binding regions, we have now characterized the sites of methylation that occur when calmodulin is incubated in buffers with or without the calcium chelator ethylene glycol bis($\beta$-aminoethyl ether)-*N*,*N*,*N*′,*N*′-tetraacetic acid (EGTA). Calmodulin was treated at pH 7.4 for 13 days at 37 °C under these conditions and was then methylated with erythrocyte D-aspartyl/L-isoaspartyl methyltransferase isozyme I and *S*-adenosyl-L-[*methyl*-$^3$H]methionine. The $^3$H-methylated calmodulin product was purified by reverse-phase HPLC and digested with various proteases including trypsin, chymotrypsin, endoproteinase Lys-C, clostripain, and *Staphylococcus aureus* V8 protease, and the resulting peptides were separated by reverse-phase HPLC. Peptides containing Asp-2 and Asp-78, as well as calcium binding sites II, III, and IV, were found to be associated with radiolabel under these conditions. When calmodulin was incubated under the same conditions in the presence of calcium, methylation at residues in the $Ca^{2+}$ binding regions was not observed. These results suggest that there may be a correlation between the flexibility of polypeptide segments and the potential of their aspartyl and asparaginyl residues to undergo degradation via succinimide-linked reactions.

Protein carboxyl methyltransferase type II catalyzes the transfer of methyl groups from *S*-adenosylmethionine into ester linkages in peptides and proteins at altered aspartyl residues, including D-aspartate and L-isoaspartate. These residues appear to originate from the spontaneous decomposition of proteins via succinimide intermediates, and this methylation reaction may play a role in the repair or degradation of these damaged proteins (McFadden & Clarke, 1982; Clarke, 1985; Johnson et al., 1987; Galletti et al., 1988; O'Connor & Yutzey, 1988). To understand the factors involved in the formation of L-isoaspartyl and D-aspartyl residues, we mapped the sites of methylation in bovine brain calmodulin, an $M_r$ 17 000 protein that mediates the effects of $Ca^{2+}$ on cellular metabolism [for reviews, see Manalan and Klee (1984) and Wang et al. (1985)]. We found that L-isoaspartyl residues originating from aspartyl residues at the 2- and 78-positions were major sites of methylation in affinity-purified calmodulin (Ota & Clarke, 1989a). These residues are located in two apparently flexible regions of the protein; one near the N-terminus (Babu et al., 1988) and one at a seven-turn $\alpha$-helical region that connects the two globular domains (Babu et al., 1988; Bayley et al., 1988; Persechini & Kretsinger, 1988). We suggested that the segmental flexibility of the polypeptide chain might allow succinimide formation.

Recently, it was found that incubation of calmodulin under physiological conditions of temperature and pH in the absence of calcium resulted in an increase in its methyl-accepting capacity (Johnson et al., 1987, 1989). We have now mapped the locations of methylation sites after calmodulin was incubated under similar conditions in the presence or absence of calcium. Incubation under either condition results in an increase in the methyl acceptor capacity of sites originating from Asp-2 and Asp-78 relative to unincubated material. Significantly, incubation in the absence of calcium produces new

† This work was supported by Grant DMB-8602102 from the National Science Foundation. I.M.O. was supported in part by U.S. Public Health Service Training Grant GM 07185.

* Address correspondence to this author at the Department of Chemistry and Biochemistry, University of California.

0006-2960/89/0428-4020$01.50/0 